Lab on a Chip

View Online
Dynamic Article Links

Cite this: *Lab Chip*, 2011, **11**, 385

www.rsc.org/loc

COMMUNICATION

Addressable electrode array device with IDA electrodes for high-throughput detection†

Kosuke Ino,*[a] Wataru Saito,[a] Masahiro Koide,[ab] Taizo Umemura,[a] Hitoshi Shiku[a] and Tomokazu Matsue*[a]

Received 23rd September 2010, Accepted 25th November 2010
DOI: 10.1039/c0lc00437e

Published on 13 December 2010 on http://pubs.rsc.org | doi:10.1039/C0LC00437E
Downloaded by Library of Chinese Academy of Sciences on 28 January 2011

An electrochemical device is proposed for high-throughput electrochemical detection that consists of 32 row and 32 column electrodes on a single glass substrate. The row and column electrodes are connected to interdigitated array (IDA) electrodes to form 1024 (32 × 32) addressable sensor points in the device. Electrochemical responses from each of the 1024 sensors were successfully acquired on the device within 1 min using redox cycling at individual IDA electrodes, which ensures application of the device to comprehensive, high-throughput electrochemical detection for enzyme-linked immunosorbent assay (ELISA), reporter gene assay for monitoring gene expressions, and DNA analysis.

Recently, the development of array-based biosensors has received a great deal of attention due to the strong demand for rapid, comprehensive, and high-throughput analyses. These techniques take advantage of the two-dimensional layout of recognition elements to allow simultaneous detection and quantification of multiple analytes. Many array-based biosensors are based on fluorescence detection, because fluorescence measurements typically have high sensitivity and a variety of tools for performing the measurements are commercially available. However, fluorescence detection has some disadvantages, such as undesired fluctuations due to quenching or emission from non-target materials, shielding by turbid solution, and the need to label non-fluorescent species, which may cause toxic side effects during analyses. As an alternative method, electrochemical detection has also been incorporated into biosensor devices. The electrochemical signal can be processed by conventional electronics in a very cheap and fast manner. Furthermore, miniaturized electrochemical transducers can easily be integrated in a microsystem by employing conventional microfabrication technologies. In the past decade, various types of amperometric microelectrode arrays have been designed and applied to chemical and biological analyses. These electrochemical array devices have substantial advantages, including rapid response time and qualitative and quantitative detection.[1,2]

[a]*Graduate School of Environmental Studies, Tohoku University, Sendai, Japan. E-mail: matsue@bioinfo.che.tohoku.ac.jp; ino.kosuke@bioinfo.che.tohoku.ac.jp*
[b]*Environmental Chemistry Division and Research Center for Environmental Risk, National Institute for Environmental Studies, Tsukuba, Japan*

† Electronic supplementary information (ESI) available: Fig. S1–S4. See DOI: 10.1039/c0lc00437e

Among the various electrochemical arrays, the development of an individually addressable device has been recognized as a key issue to cope with increasing demands for a versatile, reliable and easy-to-use analytical system, especially for comprehensive screening purposes.[3,4] However, it is difficult to collect electrochemical responses at many individual measurement points using a conventional electrochemical device, because sufficient space for the bond pads is not available on the chip border. To solve this problem, we have proposed a novel method to realize individually addressable electrochemical measurement using a device consisting of two sets of microelectrode arrays.[5–8] In the device, two arrays of band microelectrodes are arranged orthogonally face-to-face to fabricate an $n \times n$ array of crossing points (measurement points) with only $2n$ bonding pads for external connection. The crossing points of the column and row electrodes can easily be addressed by setting the potentials at the column and row electrodes to appropriate values. This addressable and multiple detection system has been applied for the detection of enzyme activity[8] and the expression of reporter proteins,[7] and for cell imaging.[5] Although the device is very useful for high-throughput electrochemical detection, careful assembly of the device is required to align two different glass substrates with the row or column electrodes at exact locations upon each measurement, which is time-consuming and results in low reproducibility. Furthermore, there is no open space on the device for handling samples such as cells, because the sensor areas are surrounded by glass substrates with electrodes. In this study, we have developed a new device to solve these problems. The general architecture, outlined in Fig. 1, provides a means for creating a new detection system that enables electrochemical detection based on local redox cycling and 1024 addressable sensor points incorporated into a small area (40 mm^2) for the comprehensive imaging of electrochemical species.

Interdigitated array (IDA) electrodes were incorporated onto glass substrates to arrange a single IDA at each sensor point of the device. IDA electrodes have two interdigitated comb-type arrays, each of which consists of planar and parallel metal fingers.[9] When the potential of each comb-type electrode is appropriately controlled, a species oxidized at an electrode finger can be reduced back at the neighboring fingers, resulting in redox cycling for amplification of the electrochemical signal. In this study, one comb-type electrodes of the IDA connected to a column electrode and the other to a row electrode.

As a first processing step, Ti/Pt was sputtered on glass substrates (50 × 26 mm) to fabricate the row electrodes and IDAs (Fig. 2a and

View Online

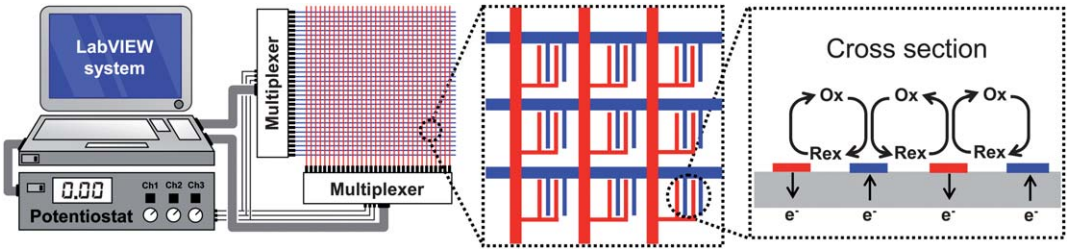

Fig. 1 Schematic illustration of local redox cycling-based electrochemical detection. The device consists of 32 column and 32 row electrodes. The column electrodes are perpendicular to the row electrodes and an IDA is fabricated in each microwell located at the individual crossing points. A potentiostat is connected to these electrodes through a multiplexer and the instruments are controlled with a computer. Local redox cycling is induced only at the IDAs located at designated cross points. Red and blue electrodes indicate column and row electrodes, respectively.

Downloaded by Library of Chinese Academy of Sciences on 28 January 2011
Published on 13 December 2010 on http://pubs.rsc.org | doi:10.1039/C0LC00437E

S1a†). A row electrode was connected to one comb-type electrode of the IDA. The row electrodes were insulated with SU-8 (thickness, 2 μm) (Fig. 2b and S1b†) for separation of the row and column electrodes and then Ti/Pt was sputtered on the substrates to fabricate a column electrode connected to the other comb-type electrode of the IDA (Fig. 2c and S1c†). Finally, the column electrodes were insulated with SU-8 (thickness, 5 μm) to fabricate arrays of measurement microwells with exposed IDAs (Fig. 2d and S1d†). The device consisted of 32 row electrodes and 32 column electrodes to form 1024 sensor points with microwells (length: 100 μm, width: 100 μm, height: 7 μm) (Fig. 2). Each individual IDA can function as an independent electrochemical sensor, and 1024 sensor microwells were incorporated into a small area (approximately 40 mm^2) (Fig. 2e). The images of the IDAs show that the width of each electrode finger and the gap between the fingers are approximately 8 and 12 μm, respectively (Fig. 2g and h). Unlike the previous assembly, the present device has the row/column electrodes and resulting sensor wells placed on a single substrate. Since the sensor well with IDA has a wide opening, a sample solution containing analyte materials can easily be introduced into the device and recovered after the measurement.

Clip connectors (CCNL-050-37-FRC, Yokowo, Tokyo, Japan) were connected to the device for multipoint electrochemical detection (ESI, Fig. S2†). The clip connectors were installed to multiplexers (NI

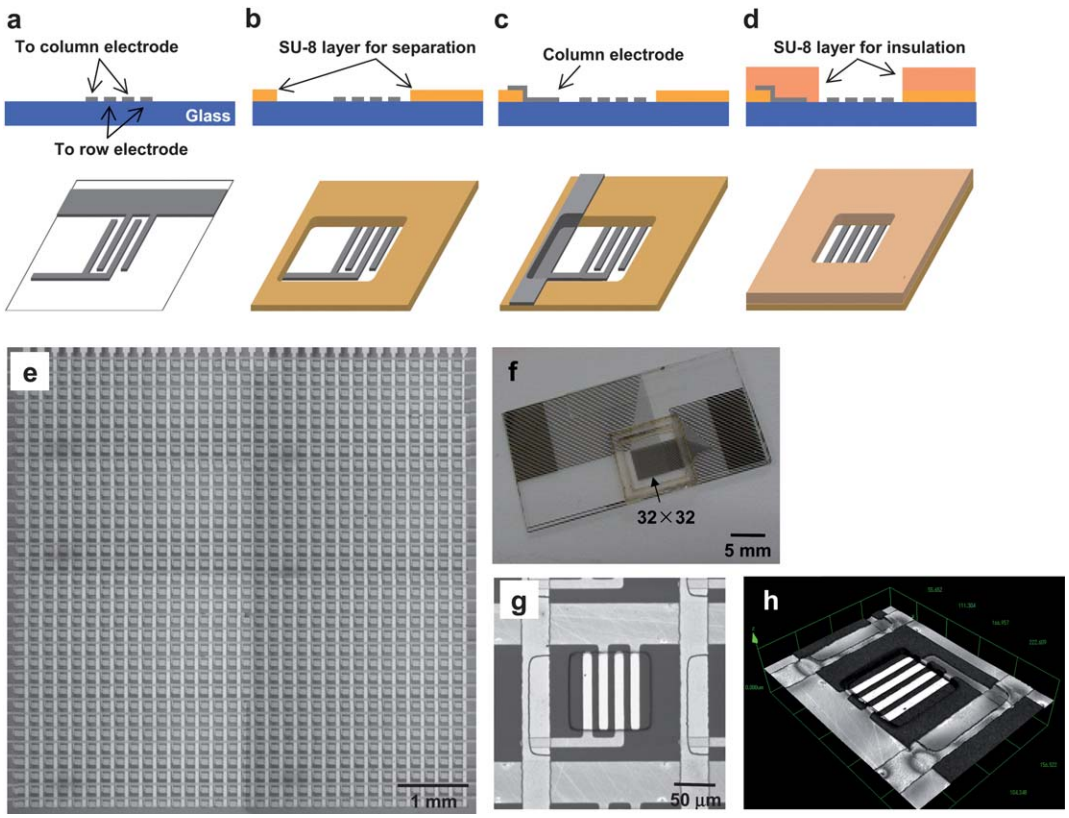

Fig. 2 (a–d) Schematic illustration of the device fabrication process. (a) Ti/Pt is sputtered on a glass substrate to fabricate the row electrodes and IDAs. (b) The insulation layer (SU-8) is fabricated on the substrate to separate the row and column electrodes. (c) Ti/Pt is sputtered on the substrate to form the column electrodes. (d) A second SU-8 layer insulates the sensor microwells. Images of (e and f) the 32 × 32 crossing points, and (g and h) the sensor point. An acrylic frame was placed on the device for keeping sample solutions on the sensor points (f).

 This journal is © The Royal Society of Chemistry 2011

View Online

Published on 13 December 2010 on http://pubs.rsc.org | doi:10.1039/C0LC00437E
Downloaded by Library of Chinese Academy of Sciences on 28 January 2011

PXI-2529, National Instruments, Austin, TX) and a multichannel potentiostat (HA-1010 mM4, Hokuto Denko, Tokyo, Japan) to control the voltage applied to the electrodes. Voltage control and data collection were performed using an AD/DA converter (PXI-6723, National Instruments) through a program written with LabVIEW. Sample solution was introduced onto the device, and an Ag/AgCl reference electrode and a Pt counter electrode were inserted into the sample solution (ESI, Fig. S2†).

Ferrocenemethanol (FMA), a redox compound showing reversible electrochemical behavior, was used to evaluate the device. Fig. 3a shows the amperograms of 4.0 mM FMA in a buffer solution (0.1 M KCl, 25 mM KH_2PO_4 and 25 mM Na_2HPO_4) at a sensor point. The oxidation current at the column electrode was divided by 32 to calculate the current based on redox cycling at a single sensor point. The amperograms at the column electrode (generator) show a transient spike upon the potential step from 0.00 to 0.50 V and then reach a steady-state current for oxidation of FMA. The reduction current at the row electrode (collector) set at 0.00 V increased immediately at the potential step and reached a steady-state, which indicates that FMA^+ generated at the column electrode was reduced at the row electrode. The collection efficiency (the ratio of reduction current at the row electrode to oxidation current at the column electrode at steady-state) was found to be approximately 50% (Fig. 3a). The electrochemical response reached a steady state within 1000 ms after the potential step (Fig. 3a), so the period for precondition was set at 1000 ms (ESI, Fig. S3†). The electrochemical signals at the individual sensors were proportional to the concentration of FMA (Fig. 3b). *p*-Aminophenol (*p*AP), a redox compound showing reversible electrochemical behavior, was also detected, and concentration-dependent electrochemical signals were acquired.

The scanning process was automatically performed using a program written with LabVIEW, as described in our previous paper[8] and Fig. S3†. Electrochemical responses at the 1024 sensors were collected by sequentially changing the potential applied to the column and row electrodes, allowing the system to be addressable within 1 min (ESI, Fig. S3†). As a demonstration of multipoint addressable electrochemical detection, designated sensor microwells were coated with bovine serum albumin (BSA) membrane. A mixture of 1.0 mg BSA, 15 mL of water, and 2 mL of 5% glutaraldehyde (GA) was prepared and dropped onto some of the sensor microwells. The character "ON" was drawn on the device with the BSA mixture, and the FMA solution was then introduced into the device. After adding the FMA solution, the electrochemical signals at the individual sensors were acquired. The BSA membranes blocked the redox cycling of FMA/FMA^+, so the electrochemical responses at the designated microwells were significantly decreased compared with the uncoated microwells (Fig. 3c). These results show that the device can be applied to multipoint addressable electrochemical detection. Fig. 3c also shows that the redox component diffusion between the sensor wells was slight during measurements since the current at the

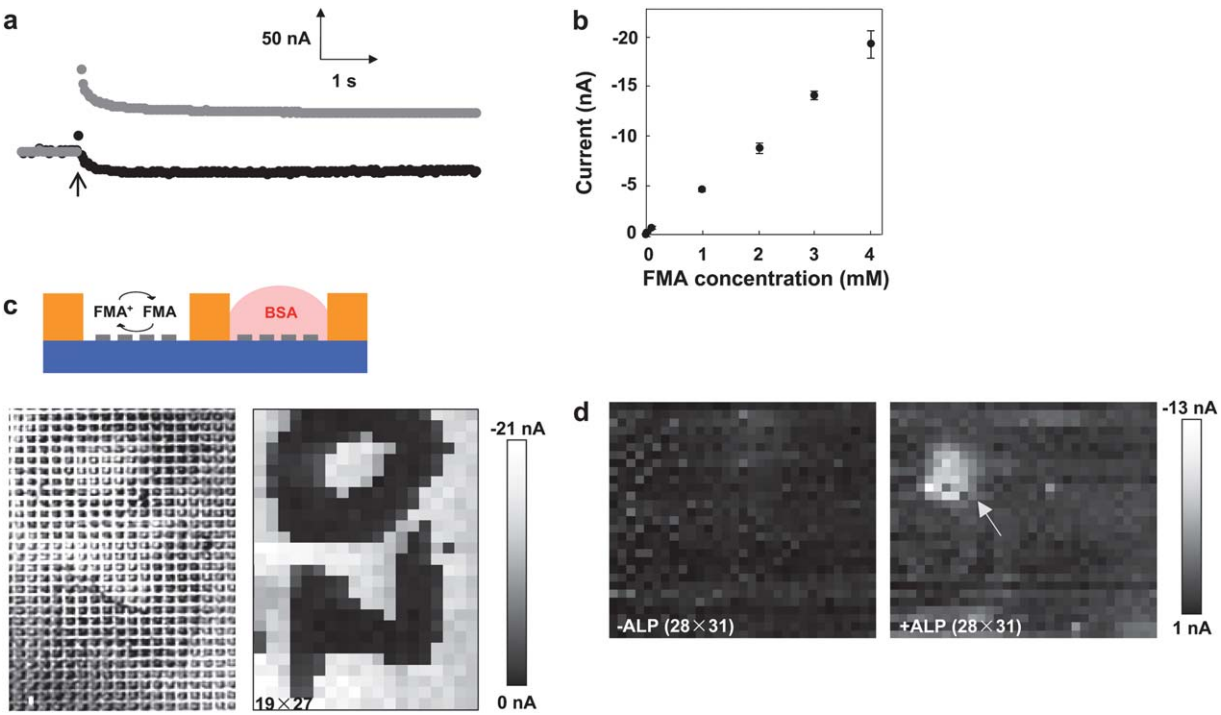

Fig. 3 (a) Amperograms of 4.0 mM FMA observed at the device. Responses from the oxidation of FMA and the reduction of FMA^+ obtained at the column electrode (generator electrode, gray symbol) and row electrode (collector electrode, black symbol), respectively. The column electrode was stepped from 0.00 to 0.50 V at the time indicated by the arrow, while the row electrode was held at 0.00 V. (b) Dependence of the electrochemical signals on the FMA concentration (0.01–4 mM). The signal was detected at the row electrodes 1 s after the potential step of the column electrodes from 0.00 to 0.50 V. Data points represent the mean ± SD of four-six independent experiments. (c) Schematic illustration showing the blocking effect of BSA membrane on the redox cycling of FMA/FMA^+. Microscopic imaging (bottom left) and electrochemical imaging (19 × 27 pixels) (bottom right) of the device showing the character "ON". BSA membranes efficiently blocked the redox cycling. (d) Electrochemical imaging (28 × 31 pixels) of ALP. Although no electrochemical responses were acquired before adding ALP/BSA aggregate (left image), the electrochemical response indicated by the arrow was acquired after adding the ALP/BSA aggregate (approximately 1 mm diameter) (right image).

View Online

first measurement point was similar to the current at the end measurement point.

For electrochemical imaging of enzyme, ALP and *p*APP were used. *p*APP (4.0 mM) in pH 9.0 HEPES buffer solution was introduced into the device. A mixture of 0.2 mg ALP, 1.0 mg BSA, 15 mL water, and 2 mL 5% GA was prepared, and a small amount of the mixture was added into the *p*APP solution with a syringe to make an ALP/BSA aggregate and float the aggregate on the solution. After adding the aggregate, the electrochemical signals at the individual sensors were acquired. The detection scheme for ALP is detailed in Fig. S4†. Briefly, ALP catalyzes the hydrolysis of *p*APP to yield *p*AP, which induces redox cycling,[7–10] similar to that for FMA, and provides an electrochemical image. This redox cycling between the anode and cathode amplifies the electrochemical signal from *p*AP produced by ALP. The image followed the position of the ALP/BSA aggregate in the solution and the intensity was dependent on the ALP activity of the aggregate (Fig. 3d). After moving the ALP/BSA aggregate, the electrochemical signals from ALP were also moved. Enzymes, such as ALP, were successfully detected using the device; therefore, this device could be used as a comprehensive, high-throughput lab-on-a-chip tool for applications such as enzyme-linked immunosorbent assay (ELISA), reporter gene assay for monitoring gene expressions, DNA analysis, and cell culture array. Although an application of electrochemical potentials to electrodes may be a critical issue for adhesive cells, it is unnecessary to bound cells on the electrodes of the device since the device has microwells that can trap cells or spheroids on the sensors for cell assays.

In conclusion, a multipoint addressable electrochemical device with a high density of sensor points was proposed. 32 row and 32 column electrodes were incorporated into the device. An IDA was fabricated in each microwell located at each of the crossing points of the row and column electrodes, which resulted in the formation of 1024 addressable sensor microwells with IDA. Electrochemical signals based on redox cycling from each of the 1024 sensors could be acquired within 1 min. This device has a wide variety of potential applications, including two-dimensional imaging of the distributions of electrochemical species. Enzymes, such as ALP, were successfully detected using the device; therefore, this device could be used as a comprehensive, high-throughput lab-on-a-chip tool for applications such as enzyme-linked immunosorbent assay (ELISA), reporter gene assay for monitoring gene expressions, and DNA analysis.

Acknowledgements

This study was supported by the Formation of Innovation Center for Fusion of Advanced Technologies, Special Coordination Funds for Promoting Science and Technology from the Ministry of Education, Culture, Sports, Science and Technology (MEXT), Japan and also by a Grant-in-Aid for Scientific Research (No. 22245011) from MEXT. This study was also supported by the Casio Science Promotion Foundation.

References

1 K. C. Cheung, P. Renaud, H. Tanila and K. Djupsund, *Biosens. Bioelectron.*, 2007, **22**, 1783–1790.
2 X. Xu, S. Zhang, H. Chen and J. Kong, *Talanta*, 2009, **80**, 8–18.
3 K. Dill, D. D. Montgomery, A. L. Ghindilis, K. R. Schwarzkopf, S. R. Ragsdale and A. V. Oleinikov, *Biosens. Bioelectron.*, 2004, **20**, 736–742.
4 J. H. Pei, M. L. Tercier-Waeber, J. Buffle, G. C. Fiaccabrino and M. Koudelka-Hep, *Anal. Chem.*, 2001, **73**, 2273–2281.
5 Z. Y. Lin, K. Ino, H. Shiku and T. Matsue, *Chem. Commun.*, 2010, **46**, 559–561.
6 Z. Y. Lin, K. Ino, H. Shiku, T. Matsue and G. N. Chen, *Chem. Commun.*, 2010, **46**, 243–245.
7 Z. Y. Lin, Y. Takahashi, T. Murata, M. Takeda, K. Ino, H. Shiku and T. Matsue, *Angew. Chem., Int. Ed.*, 2009, **48**, 2044–2046.
8 Z. Lin, Y. Takahashi, Y. Kitagawa, T. Umemura, H. Shiku and T. Matsue, *Anal. Chem.*, 2008, **80**, 6830–6833.
9 O. Niwa, Y. Xu, H. B. Halsall and W. R. Heineman, *Anal. Chem.*, 1993, **65**, 1559–1563.
10 B. Elsholz, R. Wörl, L. Blohm, J. Albers, H. Feucht, T. Grunwald, B. Jürgen, T. Schweder and B. Hintsche, *Anal. Chem.*, 2006, **78**, 4794–4802.

Downloaded by Library of Chinese Academy of Sciences on 28 January 2011
Published on 13 December 2010 on http://pubs.rsc.org | doi:10.1039/C0LC00437E

 This journal is © The Royal Society of Chemistry 2011